academicJournals

Vol. 8(21), pp. 890-901, 4 June, 2013
DOI 10.5897/SRE11.2225
ISSN 1992-2248 ©2013 Academic Journals
http://www.academicjournals.org/SRE

Scientific Research and Essays

Full Length Research Paper

Theoretical analysis on the laminar flow of an elastico-viscous fluid between a moving elliptic plate with constant injection and the ground

Serdar Barış[1] and M. Salih Dokuz[2]*

[1]Faculty of Engineering, Department of Mechanical Engineering, Istanbul University, Avcılar 34320, Istanbul, Turkey.
[2]Faculty of Mechanical Engineering, Istanbul Technical University, Gümüşsuyu 34437, Istanbul, Turkey.

Accepted 17 May, 2013

A theoretical study is presented for the problem of injection of an elastico-viscous fluid through a moving elliptic plate. The governing equations are reduced to a system of nonlinear ordinary differential equations by means of appropriate transformations for the velocity components. The resulting boundary value problem is solved numerically using the Matlab solver singular boundary value problem (SBVP). The current numerical analysis encompasses the range of cross-flow Reynolds number *R* as $0 \le R \le 5$. The results are compared with those known from the literature and an excellent agreement is found. Perturbation solutions are also obtained for small *R*. A comparison of the numerical solutions with the perturbation solutions is made. The comparison shows that the perturbation solutions give acceptable results for $R < 1$ and $N < 0.2$, where *N* is the viscoelastic fluid parameter. The influence of the viscoelastic fluid parameter on the velocity, load-carrying capacity and friction force has been examined carefully.

Key words: Elasticoviscous fluid, porous slider, load-carrying capacity, friction force.

INTRODUCTION

The flow of Newtonian and non-Newtonian fluids through porous channels has relevance to several technologically significant problems. Examples of these are the cases of boundary layer control, transpiration cooling, and gaseous diffusion. In addition to applications mentioned above, blowing is used to add reactants, prevent corrosion and reduce the drag. Suction is applied to chemical processes to remove reactants (Schlichting, 1968; Skalak, 1978). The case of a two-dimensional, incompressible, steady, laminar suction flow of a Newtonian fluid in a parallel-walled porous channel was first studied by Berman (1953). He solved the Navier-Stokes equations using a perturbation method for very low cross-flow Reynolds number. After his pioneering work, the flow of fluids over porous boundaries has been studied by many researchers (Sellars, 1955; Yuan, 1956; White et al., 1958; Proudman, 1960; Terrill and Shrestha, 1965; Brady, 1984; Cox, 1991; Singh, 1993; Choi et al., 1999; Bujurke et al., 2000; Ariel, 2002; Fang, 2004; Kurtcebe and Erim, 2005; Kamisli, 2006).

In this study, a numerical solution of the steady flow of an elastico-viscous fluid between a porous elliptic plate and the ground is given. The computer program utilized in the present research is the Matlab solver singular boundary value problem (SBVP). To the best of our knowledge, the results of this paper are new and they have not been published before. The calculation of such flows is interesting in the mechanical engineering

*Corresponding author. E-mail: dokuzme@itu.edu.tr. Tel:+902122931300. Fax: +902122450795.

research for some developments concerning fluid-cushioned porous sliders. It is well-known fact that fluid-cushioned porous sliders are useful in reducing the frictional resistance of moving objects (Bruce, 2012; Keith et al., 2012). For Newtonian fluids, previous studies include the porous circular slider (Wang, 1974), the porous flat slider (Skalak and Wang, 1975), and the porous elliptic slider (Wang, 1978; Watson et al., 1978). Later, the fluid dynamics of a porous elliptic slider was studied by Bhatt (1981) for a second-order viscoelastic fluid. He obtained the first-order perturbation solution in terms of cross-flow Reynolds number. Ariel (1993) has extended Skalak and Wang's (1975) analysis to a Walters'B viscoelastic fluid which is characterized by two material constants. In his study, the perturbation and exact numerical solutions have been obtained. The numerical solutions in the present paper include those given by Ariel (1993) as a special case. Also, for the case of Newtonian fluid, there is an overlap between our results and those given in Wang (1974), Skalak and Wang (1975), Wang (1978) and Watson et al. (1978). These give us confidence regarding analytical and numerical calculations. Bhatt's (1981) work was extended by Barış (2002) to the case of a Walters'B fluid but the author disregarded a very important issue about substantiating the reliability of the perturbation solutions, and hence he failed to explicitly highlight the validity of the perturbation solutions for the problem under investigation. The exact numerical solutions presented in this paper pointed out that the perturbation technique does not guarantee producing of the correct results qualitatively or quantitatively. Recently, Elsharkawy and Alyaqout (2009) proposed an approach for designing the optimum shape of slider bearing using sequential quadratic programming. Khan et al. (2011a) obtained a series solution of the long porous slider problem using the homotopy perturbation method. In their subsequent research, they solved the long porous slider problem using the Adomian decomposition method (Khan et al., 2011b). Shukla and Deheri (2011) analyzed the performance of a porous rough secant shaped slider bearing under the presence of a magnetic fluid lubricant. Faraz (2011) studied the circular porous slider problem using variational iteration algorithm-II. More recently, Wang (2012) studied the effect of slip on the performance of the porous slider. Shah et al. (2012) theoretically discussed about the inclined slider bearing with porous layer attached to slider as well as stator including effects of slip velocity and squeeze velocity. Ghoreishi et al. (2012) obtained the approximate solution for the problem of circular porous slider using one step optimal homotopy analysis method.

MATERIALS AND METHODS

Formulation of the problem

We consider the steady, incompressible, laminar flow of an elastico-viscous fluid between a porous elliptic plate and the ground. Figure 1 shows the physical model and the coordinate system. A fluid is injected through an elliptic plate, boundary of which is described by $x^2 + \beta y^2 = D^2 \ \ (\beta < 1)$, *z=d*, where β is the square of the ratio of minor axis to major axis. The supply pressure is assumed to be large enough to cause a nearly constant injection velocity U_3 through the elliptic plate. The porous elliptic plate is moving laterally with velocities U_1 and U_2 along the negative x- and y- directions, respectively. We have further assumed the gap width *d* between the elliptic plate and the ground is small compared with *D*, that is, $D >> d$. Due to this assumption the edge effects can be ignored.

The major axis of the elliptic plate under consideration is the segment of length $2D/\sqrt{\beta}$ between the y-intercepts $(0, \pm D/\sqrt{\beta})$. The minor axis is the segment of length *2D* between the x-intercepts $(\pm D, 0)$. Its eccentricity $e = \sqrt{1-\beta}$, which indicates the degree of departure from circularity, may vary from 0 to 1. Note that our current results reduce the circular case when *e = 0*, that is, $\beta = 1$, and the flat case when *e = 1*, that is, $\beta = 0$. As a result, the solutions presented in this research include the special cases corresponding to a porous circular plate and a porous flat plate.

There are many fluids whose behavior cannot be described by the classical Navier-Stokes equations. The inadequacy of the theory of Newtonian fluids in predicting the behavior of some fluids, especially those with high molecular weight, leads to the developments of non-Newtonian fluid mechanics. There are numerous models of viscoelastic fluids suggested in the literature. To get some insight into their flow behavior, it is preferable to restrict to a model with a minimum number of parameters in the constitutive equations. We have chosen the model of elastico-viscous fluid for our study as it involves only one non-Newtonian parameter. The Cauchy stress tensor **T** in such a fluid has the form (Beard and Walters, 1964).

$$\mathbf{T} = -p\mathbf{I} + 2\eta_0\mathbf{e} - 2k_0\frac{\delta \mathbf{e}}{\delta t} \tag{1}$$

in which *p* is the pressure, I is the identity tensor, and the rate of strain tensor e is defined by

$$2\mathbf{e} = \nabla\mathbf{v} + (\nabla\mathbf{v})^T, \quad (\nabla\mathbf{v})^{ij} = \partial v_j / \partial x_i \tag{2}$$

where **v** is the velocity vector, ∇ is the gradient operator, and $\delta / \delta t$ denotes the convected differentiation of a tensor quantity in relation to the material in motion. For the rate of strain tensor, it is given by

$$\frac{\delta \mathbf{e}}{\delta t} = \frac{\partial \mathbf{e}}{\partial t} + \mathbf{v}\cdot\nabla\mathbf{e} - \mathbf{e}\cdot\nabla\mathbf{v} - (\nabla\mathbf{v})^T\cdot\mathbf{e} \tag{3}$$

Finally η_0 and k_0 are, respectively, the limiting viscosity at small rate of shear and the short memory coefficient. For a detailed description of this model the reader should consult Beard and Walters (1964). From the theoretical point of view, there has been a

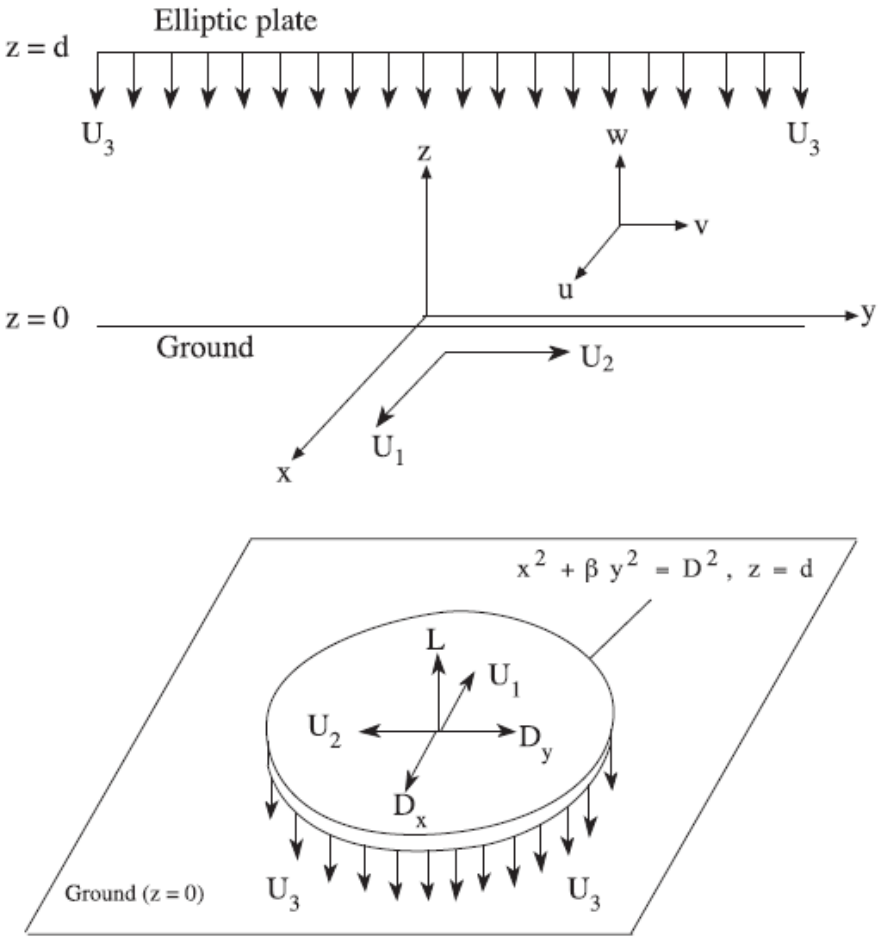

Figure 1. Sketch of flow geometry and coordinate system.

remarkable interest in the study of Walters' B elastico-viscous fluid in recent times. Calculations based on this fluid model for various flow problems have been carried out by many authors (Nandeppanavar et al., 2010; Singh et al., 2010; Joneidi et al., 2010; Gupta and Aggarwal, 2011; Ghasemi and Bayat, 2011; Tonekaboni et al., 2012; Prakash et al., 2012).

In addition to Equation (1), the basic equations of the problem are the following:

Continuity equation:

$$\nabla \cdot \mathbf{v} = 0 \tag{4}$$

Equations of motion:

$$\rho(\mathbf{v} \cdot \nabla \mathbf{v}) = \nabla \cdot \mathbf{T} \tag{5}$$

where ρ is the density. The assumptions made in the above equations are as follows: (a) The flow is steady and laminar, (b) The fluid is incompressible, (c) The body forces are negligible.

Substituting Cauchy stress tensor from Equation (1) into equations of motion (5), with the aid of Equations (2) and (3), we get

$$\rho(\mathbf{v} \cdot \nabla \mathbf{v}) = -\nabla p + \eta_0 \nabla^2 \mathbf{v} - 2k_0 \mathbf{v} \cdot \nabla \nabla^2 \mathbf{v} + k_0 \nabla^2 (\mathbf{v} \cdot \nabla \mathbf{v}) \tag{6}$$

In a reference frame translating with the porous elliptic plate, let *u*, *v*, and *w* be the velocity components corresponding to the x-, y- and z- directions, respectively. Following Wang (1978), we look for a solution, compatible with the continuity Equation (4), of the form

$$u = U_1 f(\eta) + \frac{U_3 x}{d} h'(\eta), \quad v = U_2 g(\eta) + \frac{U_3 y}{d} k'(\eta), \quad w = -U_3 (h(\eta) + k(\eta)) \tag{7}$$

where $\eta = z / d$ is the similarity variable and the prime denotes the differentiation with respect to η.

The boundary conditions for the velocity field are

$$u(0) = U_1, \quad v(0) = U_2, \quad w(0) = 0, \quad u(1) = 0, \quad v(1) = 0, \quad w(1) = -U_3 \tag{8}$$

By using equations of motion (6) and similarity transformation (7), it can be shown that the general expression for the pressure distribution is

$$p(x, y, \eta) = C_1 y + C_3 x + C_2 \frac{y^2}{2} + C_4 \frac{x^2}{2} - \frac{1}{2}\rho w^2 + \eta_0 \frac{dw}{dz} + 2k_0 \left(\frac{dw}{dz}\right)^2 - k_0 w \frac{d^2 w}{dz^2} + p_0, \tag{9}$$

where the constants C_1, C_2, C_3 and C_4 are

$$C_1 = \frac{\eta_0 U_2}{d^2}(g'' + R[(h+k)g' - k'g] + RN[(h+k)g''' - (k' + 2h')g'' + (k'' - h'')g' - k'''g]), \quad (10)$$

$$C_2 = \frac{\eta_0 U_3}{d^3}(k''' + R[(h+k)k'' - k'^2] + RN[(h+k)k^{IV} - 2(h' + k')k''' - h''k'' + k''^2]), \quad (11)$$

$$C_3 = \frac{\eta_0 U_1}{d^2}(f'' + R[(h+k)f' - h'f] + RN[(h+k)f''' - (h' + 2k')f'' + (h'' - k'')f' - h'''f]), \quad (12)$$

$$C_4 = \frac{\eta_0 U_3}{d^3}(h''' + R[(h+k)h'' - h'^2] + RN[(h+k)h^{IV} - 2(h' + k')h''' - k''h'' + h''^2]), \quad (13)$$

and p_0 is the constant of integration. In the above equations, the cross-flow Reynolds number *R* and dimensionless measure of viscoelasticity of the fluid *N* are defined through, respectively

$$R = \frac{\rho U_3 d}{\eta_0}, \quad N = \frac{k_0}{\rho d^2} \quad (14)$$

In view of the fact that the shape of porous plate makes the isobars similar to ellipses, the constants C_1, C_2, C_3 and C_4 must satisfy the following equations:

$$C_1 = 0, \quad C_3 = 0, \quad C_2 = \beta C_4 \quad (15)$$

Substituting Equation (15) into Equations (9) to (13), we obtain

$$p(x, y, \eta) = \frac{\rho U_3^2 A}{2d^2 R}(x^2 + \beta y^2) - \frac{1}{2}\rho w^2 + \eta_0 \frac{dw}{dz} + 2k_0 (\frac{dw}{dz})^2 - k_0 w \frac{d^2 w}{dz^2} + p_0, \quad (16)$$

$$h''' + R[(h+k)h'' - h'^2] + RN[(h+k)h^{IV} - 2(h' + k')h''' - k''h'' + h''^2]) = A, \quad (17)$$

$$k''' + R[(h+k)k'' - k'^2] + RN[(h+k)k^{IV} - 2(h' + k')k''' - h''k'' + k''^2]) = \beta A, \quad (18)$$

$$f'' + R[(h+k)f' - h'f] + RN[(h+k)f''' - (h' + 2k')f'' + (h'' - k'')f' - h'''f]) = 0, \quad (19)$$

$$g'' + R[(h+k)g' - k'g] + RN[(h+k)g''' - (k' + 2h')g'' + (k'' - h'')g' - k'''g]) = 0, \quad (20)$$

where *A* is an unknown constant. The boundary conditions on velocity given by Equation (8) require

$$h(0) = h'(0) = h'(1) = 0, \quad k(0) = k'(0) = k'(1) = 0, \quad h(1) + k(1) = 1, \quad f(0) = 1, \quad f(1) = 0, \quad g(0) = 1, \quad g(1) = 0. \quad (21)$$

The above boundary value problem includes the special cases corresponding to a porous flat plate and a porous circular plate. As far as practical applications are concerned, it is important to know the governing equations related to the above mentioned special cases. They can be easily obtained from Equations (17) to (21) by letting $\beta = 0, k \equiv 0$, and $\beta = 1, g \equiv 0, h \equiv k$, respectively, as follows:

Porous flat plate

$$h''' + R(hh'' - h'^2) + RN(hh^{IV} - 2h'h''' + h''^2) = A \quad (22)$$

$$f'' + R(hf' - h'f) + RN(hf''' - h'f'' + h''f' - h'''f) = 0 \quad (23)$$

$$g'' + Rhg' + RN(hg''' - 2h'g'' - h''g') = 0 \quad (24)$$

with the boundary conditions

$$h(0) = h'(0) = h'(1) = 0, \quad h(1) = 1, \quad f(0) = 1, \quad f(1) = 0, \quad g(0) = 1, \quad g(1) = 0 \quad (25)$$

Porous circular plate

$$h''' + R(2hh'' - h'^2) + RN(2hh^{IV} - 4h'h''') = A \quad (26)$$

$$f'' + R(2hf' - h'f) + RN(2hf''' - 3h'f'' - h'''f) = 0 \quad (27)$$

with the boundary conditions

$$h(0) = h'(0) = h'(1) = 0, \quad h(1) = 1/2, \quad f(0) = 1, \quad f(1) = 0 \quad (28)$$

It is also recorded that for a Newtonian fluid, Equations (16) – (21) are the same as those obtained by Wang (1978).

It is interesting to determine the effect of the non-dimensional elastic parameter *N* on the shear stresses on the elliptic plate. From Equations (1) to (3) and (7), we obtain

$$T_{zx} = \frac{U_1 \eta_0}{d} f'(1) + \frac{k_0 U_1 U_3}{d^2} f''(1) + \frac{\eta_0 U_3 x}{d^2} h''(1) + \frac{k_0 U_3^2 x}{d^3} h'''(1) \quad (29)$$

$$T_{zy} = \frac{U_2 \eta_0}{d} g'(1) + \frac{k_0 U_2 U_3}{d^2} g''(1) + \frac{\eta_0 U_3 y}{d^2} k''(1) + \frac{k_0 U_3^2 y}{d^3} k'''(1) \quad (30)$$

For the problem under consideration, it is important to find the load-carrying capacity *L* and friction force components D_x and D_y. These physical quantities can be calculated by integrating pressure and shear stress components on the elliptic plate. The dimensionless expressions for the load-carrying capacity and friction force components are given through the following equations:

$$L^* = \frac{4\eta_0^2}{\rho^3 U_3^4 S D^2} \iint_S (p - p_A) dS = -\frac{1}{R^3}(h'''(0) + RN[h''^2(0) - h''(0)k''(0)]) \quad (31)$$

$$D_x^* = -\frac{1}{\rho S U_1 U_3}\iint_S T_{zx}\, dS = -\frac{f'(1)}{R} - N f''(1) \quad (32)$$

$$D_y^* = -\frac{1}{\rho S U_2 U_3}\iint_S T_{zy}\, dS = -\frac{g'(1)}{R} - N g''(1) \quad (33)$$

where p_A is the ambient pressure at the edge of the elliptic plate.

Perturbation solution

We seek the solution of Equations (17) to (20) with the boundary conditions (21) for a small cross flow Reynolds number *R*. We may expand the functions *h*, *k*, *f*, *g*, and the unknown constant *A* in a power series of *R* in the following forms:

$$h = h_0 + R h_1 + o(R^2), \quad k = k_0 + R k_1 + o(R^2), \quad f = f_0 + R f_1 + o(R^2), \quad (34)$$
$$g = g_0 + R g_1 + o(R^2), \quad A = A_0 + R A_1 + o(R^2).$$

If we substitute (34) into Equations (17) to (20), and equate the corresponding coefficients of *R* up to first order, we obtain the following set of ordinary differential equations

$$h_0''' = A_0, \quad k_0''' = \beta A_0, \quad f_0'' = 0, \quad g_0'' = 0, \quad (35)$$

$$h_1''' + (h_0 + k_0) h_0'' - h_0'^2 + N[(h_0 + k_0) h_0^{IV} - 2(h_0' + k_0') h_0''' \quad (36)$$
$$-k_0'' h_0'' + h_0''^2] = A_1,$$

$$k_1''' + (h_0 + k_0) k_0'' - k_0'^2 + N[(h_0 + k_0) k_0^{IV} - 2(h_0' + k_0') k_0''' \quad (37)$$
$$-k_0'' h_0'' + k_0''^2] = \beta A_1,$$

$$f_1'' + (h_0 + k_0) f_0' - h_0' f_0 + N[(h_0 + k_0) f_0''' - (h_0' + 2k_0') f_0'' \quad (38)$$
$$+(h_0'' - k_0'') f_0' - h_0''' f_0] = 0,$$

$$g_1'' + (h_0 + k_0) g_0' - k_0' g_0 + N[(h_0 + k_0) g_0''' - (k_0' + 2h_0') g_0'' \quad (39)$$
$$+(k_0'' - h_0'') g_0' - k_0''' g_0] = 0,$$

subject to the boundary conditions

$$h_n(0) = 0, \quad h_n'(0) = 0, \quad h_n'(1) = 0, \quad k_n(0) = 0, \quad k_n'(0) = 0, \quad k_n'(1) = 0, \quad (40)$$
$$h_0(1) + k_0(1) = 1, \quad h_1(1) + k_1(1) = 0, \quad f_0(0) = 1, \quad f_n(1) = 0, \quad f_1(0) = 0,$$
$$g_0(0) = 1, \quad g_n(1) = 0, \quad g_1(0) = 0, \quad (n = 0,1)$$

Integrating Equations (35) to (39) with the boundary conditions (40), we have

Zeroth-order solution

$$h_0 = \frac{3\eta^2 - 2\eta^3}{1+\beta}, \quad k_0 = \frac{\beta(3\eta^2 - 2\eta^3)}{1+\beta}, \quad f_0 = 1 - \eta, \quad g_0 = 1 - \eta \quad (41)$$

This solution is that of linear viscous fluid. No properties of the elastico-viscous fluid appear in Equation (41).

First-order solution

$$h_1 = \frac{16 + (84N - 1)\beta + (37 - 420N)\beta^2}{70(1+\beta)^3}\eta^2 + \frac{-27 + (504N - 18)\beta + (840N - 27)\beta^2}{70(1+\beta)^3}\eta^3 \quad (42)$$
$$-\frac{12N\beta}{(1+\beta)^2}\eta^4 + \frac{3(1 - \beta + 16N\beta)}{10(1+\beta)^2}\eta^5 + \frac{2\beta - 1}{5(1+\beta)^2}\eta^6 + \frac{2(1 - 2\beta)}{35(1+\beta)^2}\eta^7,$$

$$k_1 = \frac{(37 - 420N)\beta + (84N - 1)\beta^2 + 16\beta^3}{70(1+\beta)^3}\eta^2 + \frac{(840N - 27)\beta + (504N - 18)\beta^2 - 27\beta^3}{70(1+\beta)^3}\eta^3 \quad (43)$$
$$-\frac{12N\beta}{(1+\beta)^2}\eta^4 + \frac{3\beta(\beta - 1 + 16N)}{10(1+\beta)^2}\eta^5 + \frac{\beta(2 - \beta)}{5(1+\beta)^2}\eta^6 + \frac{2\beta(\beta - 2)}{35(1+\beta)^2}\eta^7,$$

$$f_1 = \frac{(20N - 3)(3 + \beta)}{20(1+\beta)}\eta - 3N\eta^2 + \frac{1 + 2N\beta}{1+\beta}\eta^3 + \frac{\beta - 3}{4(1+\beta)}\eta^4 + \frac{2 - \beta}{10(1+\beta)}\eta^5 \quad (44)$$

$$g_1 = \frac{(20N - 3)(1 + 3\beta)}{20(1+\beta)}\eta - 3N\eta^2 + \frac{2N + \beta}{1+\beta}\eta^3 + \frac{1 - 3\beta}{4(1+\beta)}\eta^4 + \frac{2\beta - 1}{10(1+\beta)}\eta^5 \quad (45)$$

At this level, the terms having *N* factor represent the viscoelastic character of the fluid. In a similar manner, the higher order terms can be obtained, but the calculations will become complicated. Moreover, the solutions considered are valid for only small values of *R*. Therefore, we retain up to first order terms. It is recorded that the above perturbation solutions reduce to the corresponding results for a Newtonian fluid derived by Wang (1978).

Numerical solution

Equations (17) to (20) are four simultaneous differential equations. They are fourth order in *h* and *k*, and third order in *f* and *g*. But if we put *N* = 0 (for the Newtonian case), the order of *h*, *k*, *f* and *g* is reduced by one. It would thus appear that additional boundary conditions must be imposed to obtain the solution. One of the possible methods that overcomes this requirement of additional conditions is the perturbation technique. In the absence of a means for prescribing additional boundary conditions, the perturbation method is by far the most commonly used technique in studying flows of viscoelastic fluids (Sadeghy and Sharifi, 2004; Sadeghy et al., 2005). However, there are some serious doubts regarding the reliability of the results obtained using the perturbation method when dealing with viscoelastic fluids (Ariel, 1992, 1993, 2008). That is to say that the perturbed set of equations may produce results that may be qualitatively incorrect and quantitatively inaccurate (Ariel, 1993, 1995). Therefore, the nonlinear simultaneous differential equations (17) to (20) governing the problem under discussion must be integrated numerically. However, we need four extra boundary conditions to obtain the exact numerical solution. For flows that take place in unbounded domains, it has been shown that the boundary conditions can be augmented by the fact that the solution has to be bounded or has a certain smoothness at infinity (Garg, 1994; Ariel and Teipel, 1994; Sadeghy and Sharifi, 2004; Sadeghy et al., 2005). Besides the case of the flow of viscoelastic fluids in unbounded domains, one may encounter the flow problems of viscoelastic fluids in bounded domains as in the current investigation. In such a case, one makes a reasonable assumption, namely, that all derivatives of *h*, *k*, *f* and *g* are bounded at $\eta = 0$. The physical meaning of this assumption is that the stresses and their gradients remain bounded at $\eta = 0$ (Ariel, 1994). Indeed, this is fundamental in obtaining the proper solutions of the boundary value problem given in Equations (17) to (21). Without this condition, it is easy to see that $h^{IV}(0)$, $k^{IV}(0)$, $f'''(0)$ and $g'''(0)$ become unbounded, implying that the resulting solutions would be in error near $\eta = 0$ (Ariel, 1994, 2002). With this assumption, if we set

Table 1. Comparison of the values of $f''(0)$, $g'(0)$, $h''(0)$ and $h'''(0)$ with those of Ariel (1993) in the case of a porous flat plate ($\beta = 0$) for some values of *R* and *N*.

R	*N*	$f''(0)$		$g'(0)$		$h''(0)$		$h'''(0)$	
		Present	**Ariel**	**Present**	**Ariel**	**Present**	**Ariel**	**Present**	**Ariel**
0.2	0	-1.088029	-1.088029	-1.030147	-1.030147	6.091330	6.091330	-12.465009	-12.465008
	0.1	-1.030257	-1.030257	-1.009208	-1.009208	6.093219	6.093218	-12.473985	-12.473984
	0.2	-0.964666	-0.964666	-0.986014	-0.986014	6.095284	6.095284	-12.483613	-12.483613
	0.5	-0.700942	-0.700942	-0.899598	-0.899598	6.102340	6.102339	-12.515687	-12.515686
1	0	-1.405982	-1.405982	-1.153102	-1.153102	6.454264	6.454264	-14.365857	-14.365856
	0.1	-1.155383	-1.155383	-1.029846	-1.029846	6.518076	6.518076	-14.667342	-14.667341
	0.2	-0.541463	-0.541463	-0.795851	-0.795851	6.601882	6.601881	-15.050193	-15.050191
	0.5	-3.660082	-3.660024	-0.076083	-0.076074	6.957401	6.957944	-16.642485	-16.644702
2	0	-1.744503	-1.744503	-1.309634	-1.309633	6.900850	6.900850	-16.823501	-16.823500
	0.1	-1.291448	-1.291448	-0.972443	-0.971497	7.259711	7.259711	-18.554862	-18.554860
	0.2	-5.048659	-5.048551	-0.192054	-0.191910	7.928833	7.928913	-21.711065	-21.711393

$\eta = 0$ in Equations (17) to (20) and make use of the boundary conditions at $\eta = 0$, we get

$$
\begin{aligned}
A &= h'''(0) + R\,N\,[h''^{2}(0) - k''(0)\,h''(0)],\\
k'''(0) &= \beta\,A + R\,N\,[h''(0)\,k''(0) - k''^{2}(0)],\\
f''(0) &= R\,N\,[(k''(0) - h''(0))\,f'(0) + h'''(0)],\\
g''(0) &= R\,N\,[k'''(0) + (h''(0) - k''(0))\,g'(0)].
\end{aligned}
\tag{46}
$$

It is worth mentioning that the above additional boundary conditions are essentially equivalent to the requirement that the solution reduces to the Newtonian solution as $N \to 0$. Calculations based on this assumption for various problems related to viscoelastic fluids have been carried out by some authors like Davies (1967), Frater (1970), Teipel (1986), Ariel (1992, 1994, 2002), Sadeghy and Sharifi (2004) and Mustafa et al. (2008).

The system of nonlinear ordinary differential (17) to (20) under the relevant conditions given in Equations (21) and (46) constitute a difficult two-point boundary value problem. The numerical integration of this boundary value problem is carried out using the Matlab solver singular boundary value problem (SBVP). The SBVP-package contains functions for solving boundary value problems for systems of nonlinear ordinary differential equations of the first order. The code is based on collocation at either equidistant or Gaussian collocation points. An error estimate for the global error of the approximate solution is also provided. This estimate provides the basis for an adaptive mesh selection strategy. The mesh points are automatically modified with the aim of equidistributing the global error. A detailed description is given in Auzinger et al. (2002). It is worth pointing out here that this method has been successfully used by the present authors to study the steady three-dimensional flow of a second grade fluid near the stagnation point of an infinite plate moving parallel to itself with constant velocity (Barış and Dokuz, 2006).

RESULTS AND DISCUSSION

The system of coupled ordinary differential equations (17) to (20) with the boundary conditions (21) and (46) has been solved numerically using the Matlab solver SBVP for several values of dimensionless pertinent parameters. The numerical integration proceeds as follows. The unknown initial conditions $f'(0)$, $g'(0)$, $h''(0)$, $h'''(0)$ and $k''(0)$ are roughly estimated in order to get $f''(0)$, $g''(0)$, $k'''(0)$ and the unknown constant A from Equation (46). The accuracy of the assumed missing initial conditions are checked by comparing the calculated values of $h(1)$, $k(1)$, $h'(1)$, $k'(1)$, $f(1)$ and $g(1)$ with their given values at $\eta = 1$. If a difference exists, the computations with new and improved values for the missing initial conditions are repeated. The iterative procedure is stopped when the maximum change between successive iterates is less than 10^{-5}. Since the porous sliders operate at small values of *R*, the variation of *R* is limited to a range from 0 to 5. A full numerical analysis for larger values of *R* is beyond the scope of the present work.

In order to validate the numerical method used, we have first compared our results for the values of $f''(0)$, $g'(0)$, $h''(0)$ and $h'''(0)$ with those of Ariel (1993) in Table 1 for the special case corresponding to a porous flat plate ($\beta = 0$). This table shows excellent agreement with the existing results in Ariel (1993). Moreover, the present numerical approach was validated against the results of the approximate perturbation solutions. In Tables 2 and 3, the missing initial conditions calculated from the first-order perturbation solutions are compared with the corresponding numerical solutions for several values of *R* and *N* in the case of a porous elliptic plate with $\beta = 0.5$. It is evident that the first-order perturbation solutions in terms of the *R* match almost exactly with numerical

Table 2. Variation of $f'(0)$, $f''(0)$, $g'(0)$ and $g''(0)$ with *R* and *N* using (i) approximate perturbation solution, and (ii) direct numerical solution for the case of a porous elliptic plate with $\beta = 0.5$

R	*N*	$f'(0)$		$f''(0)$		$g'(0)$		$g''(0)$	
		Pert.	**Num.**	**Pert.**	**Num.**	**Pert.**	**Num.**	**Pert.**	**Num.**
0.2	0	-1.07	-1.068881	0	0	-1.05	-1.049802	0	0
	0.1	-1.02333	-1.023794	-0.12	-0.117914	-1.01667	-1.016785	-0.12	-0.117695
	0.2	-0.976667	-0.974792	-0.24	-0.228852	-0.983333	-0.981924	-0.24	-0.221739
	0.5	-0.836667	-0.797277	-0.6	-0.524402	-0.883333	-0.864717	-0.6	-0.448610
1	0	-1.35	-1.324517	0	0	-1.25	-1.244453	0	0
	0.1	-1.11667	-1.133998	-0.6	-0.525581	-1.08333	-1.092292	-0.6	-0.528806
	0.2	-0.883333	-0.827047	-1.2	-0.876481	-0.916667	-0.887038	-1.2	-0.697068
	0.5	-0.183333	-0.207310	-3	-0.256678	-0.416667	1.699592	-3	-1.588234
2	0	-1.7	-1.607999	0	0	-1.5	-1.475829	0	0
	0.1	-1.23333	-1.346228	-1.2	-0.783380	-1.16667	-1.232768	-1.2	-0.887050
	0.2	-0.766667	5.004041	-2.4	-11.916824	-0.833333	-0.650271	-2.4	-0.980608

Table 3. Variation of $h''(0)$, $h'''(0)$, $k''(0)$ and $k'''(0)$ with *R* and *N* using (i) approximate perturbation solution, and (ii) direct numerical solution for the case of a porous elliptic plate with $\beta = 0.5$.

R	*N*	$h''(0)$		$h'''(0)$		$k''(0)$		$k'''(0)$	
		Pert.	**Num.**	**Pert.**	**Num.**	**Pert.**	**Num.**	**Pert.**	**Num.**
0.2	0	4.0419	4.042247	-8.21714	-8.218564	2.03429	2.034162	-4.10857	-4.109282
	0.1	4.03124	4.028700	-7.98248	-7.971666	2.00229	2.001003	-3.83124	-3.822995
	0.2	4.02057	4.011731	-7.74781	-7.716875	1.97029	1.964555	-3.5539	-3.533311
	0.5	3.98857	3.943251	-7.04381	-6.927184	1.87429	1.832116	-2.7219	-2.660571
1	0	4.20952	4.217399	-9.08571	-9.121430	2.17143	2.168742	-4.54286	-4.560715
	0.1	4.15619	4.093974	-7.91238	-7.655957	2.01143	1.977444	-3.15619	-2.976195
	0.2	4.10286	3.916117	-6.73905	-6.242253	1.85143	1.667334	-1.76952	-1.490583
	0.5	3.94286	1.585485	-3.21905	-0.326313	1.37143	2.487722	2.39048	-1.643034
2	0	4.41905	4.447391	-10.1714	-10.313385	2.34286	2.333520	-5.08571	-5.156692
	0.1	4.31238	4.052504	-7.82476	-6.870462	2.02286	1.858550	-2.31238	-1.730615
	0.2	4.20571	4.816364	-5.4781	-8.725169	1.70286	0.332717	0.460952	-0.077025

solutions when both *R* and *N* are small. Therefore, it can be concluded that the present code can be used with great confidence to study the problem discussed in this study.

In order to distinguish the difference between the perturbation and direct numerical solutions, an error measure for a function ϕ can be described as follows:

$$E_{\phi} = \sqrt{\frac{\sum_{i} (\phi_i^{per} - \phi_i^{num})^2}{\sum_{i} (\phi_i^{num})^2}} \qquad (47)$$

where ϕ_i^{per} denotes the perturbation solution at the space position η_i, while ϕ_i^{num} is the corresponding value obtained by the direct numerical solution. The error percentages for the similarity functions between the perturbation solutions and the numerical solutions of the boundary value problem under consideration are listed in Table 4 for different values of *R* and *N* in the case of a porous elliptic plate with $\beta = 0.5$. The table shows that the solution based on the series expansion given in Equation (34) is only valid for $R < 1$ and $N < 0.2$. For larger values of *R* and *N*, the perturbation solutions can no longer be

Table 4. Error percentages for the similarity functions *h*, *k*, *f* and *g* between the perturbation solutions and the numerical solutions in the case of a porous elliptic plate for $\beta = 0.5$ and some values of *R* and *N*.

R	*N*	E_f	E_g	E_h	E_k
0.2	0	0.079	0.034	0.138	0.142
	0.1	0.020	0.011	0.028	0.029
	0.2	0.064	0.067	0.079	0.071
	0.5	1.679	1.155	0.278	0.568
1	0	1.940	0.913	0.184	0.443
	0.1	0.714	0.505	0.625	0.636
	0.2	2.909	2.613	1.140	2.623
	0.5	17.72	57.57	79.90	45.89
2	0	7.612	3.857	0.636	1.558
	0.1	4.272	3.403	2.262	1.988
	0.2	11.61	74.63	332.1	61.08

used. In such cases, the exact numerical solutions must be used.

In Figures 2 and 3, the functions which correspond to the lateral velocity components along the x and y axes are plotted versus η for three different values of the cross flow Reynolds number *R*, with the elastic number *N* as a parameter. The elasticity of the fluid affects the lateral velocity components in different ways, depending on the chosen values of the cross flow Reynolds number. For instance, when *R*=0.2, we notice that the lateral velocity components for a viscoelastic fluid is more than those for a Newtonian fluid. However, when *R*=5, an opposite effect is observed, that is, the lateral velocity components slightly decrease with an increase in the elasticity of the fluid.

In practical applications, the primary physical quantities of interest are load-carrying capacity and friction force. Tables 5 to 7 provide the dimensionless load-carrying capacity and friction force components for various values of the parameters. It can be easily seen from these tables that for a Newtonian and viscoelastic fluid, both load-carrying capacity and friction force increase rapidly when the cross-flow Reynolds number decreases. Physically this can be explained as follows: When ρ, U_3 and η_0 are held fixed, the decrease in the value of the cross-flow Reynolds number results only from the decrease in the gap width. In this case, since the changes in the values of the velocity components occur in the smaller distance, velocity gradients become larger. For this reason, both stress components in the fluid layer and load-carrying capacity and friction force on the porous elliptic plate increase considerably as the cross-flow Reynolds number decreases.

The efficiency of a porous slider can be increased by making the ratio of friction force to load-carrying capacity smaller. As pointed out in Wang (1974, 1978), Skalak and Wang (1975) and Watson et al. (1978) the porous sliders with a Newtonian fluid should be operated at small values of the cross-flow Reynolds number for optimum efficiency. Table 5 shows that the fact that the porous sliders should be operated at values of the cross-flow Reynolds number up to unity (*R*<1) still remains valid even when a viscoelastic fluid is used. Also, we observe from Tables 5 to 7 that the ratio of friction force to load-carrying capacity increases with an increase in *R*, up to a critical value of *R* (say, R_c), in which the friction force to load-carrying capacity ratio reaches a maximum, in the interval $2 < R_c < 5$, and thereafter decreases with increasing *R*. Therefore, a porous slider should be operated beyond the critical cross-flow Reynolds number R_c that causes its efficiency to be minimum. It is noticed that for a porous flat slider, the critical cross-flow Reynolds number is approximately 4 (Skalak et al., 1975; Wang, 1978; Watson et al., 1978; Bhatt, 1981; Ariel, 1993). Finally, it can be seen from Table 7 that the friction force components become noticeably smaller as *N* is increased. Since it is aimed to reduce the frictional resistance in the lateral directions for a porous slider, it is more advantageous to design a porous slider with a viscoelastic fluid rather than a Newtonian one for the case of a large cross-flow Reynolds number.

Conclusions

In this study, we have been concerned with a theoretical investigation of the problem of a porous elliptic slider using an elasticoviscous fluid. By using the appropriate similarity transformations, the governing equations are reduced to a set of nonlinear ordinary differential equations. The boundary value problem characterizing

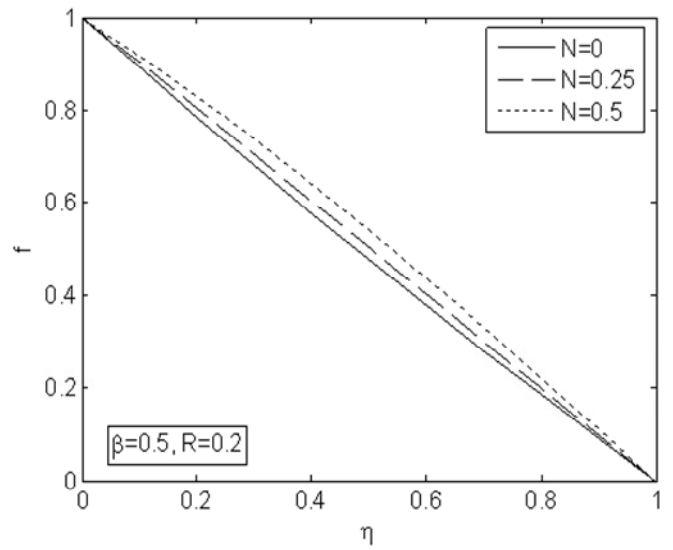

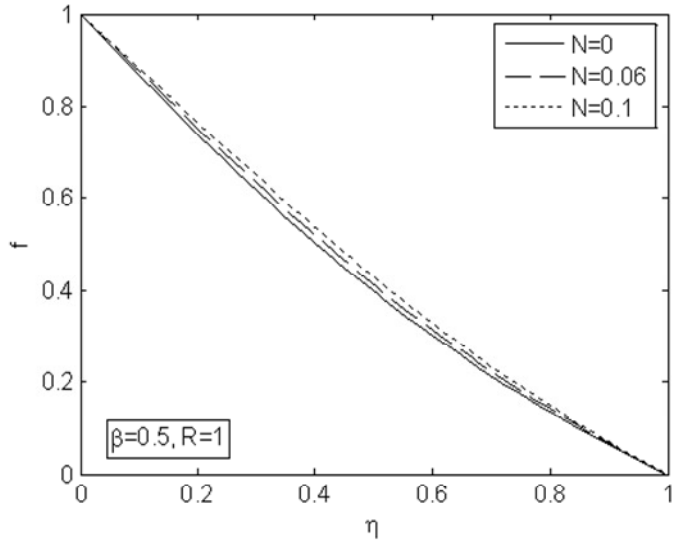

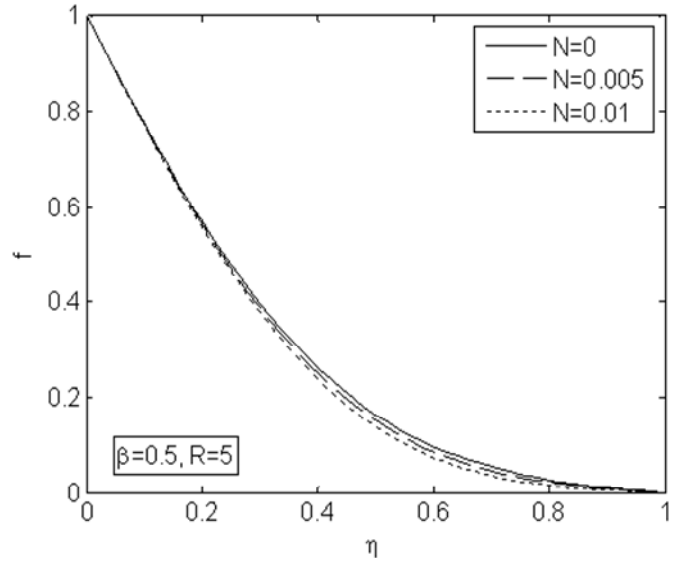

Figure 2. Lateral velocity profiles in the x-direction for $\beta = 0.5$ and some values of *R* and *N*.

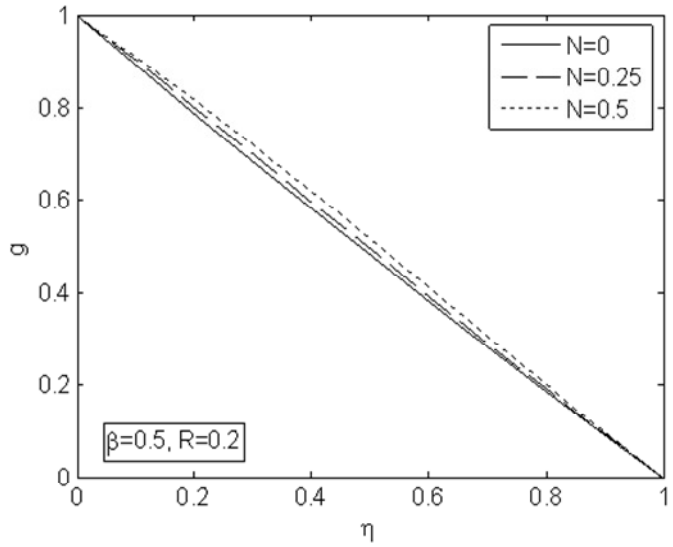

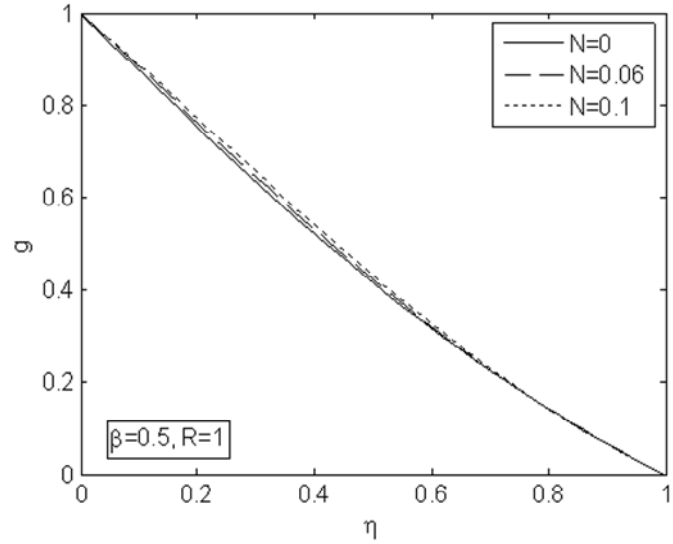

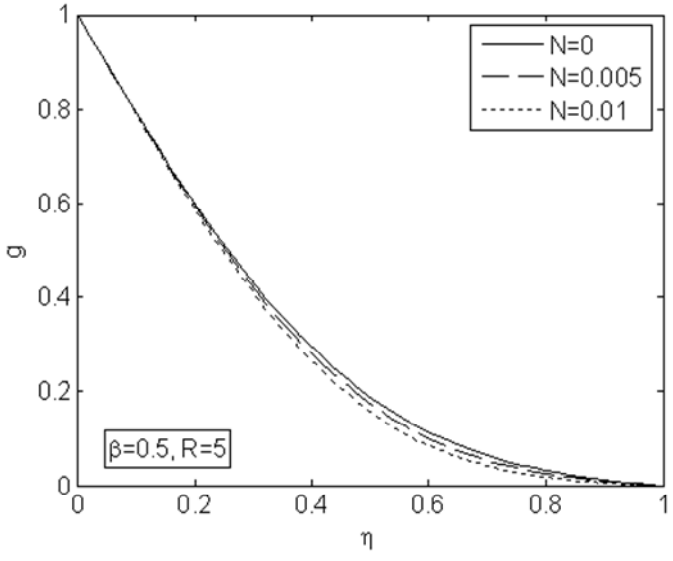

Figure 3. Lateral velocity profiles in the y-direction for $\beta = 0.5$ and some values of *R* and *N*.

Table 5. Load-carrying capacity and friction force components for R=0.2 and some values of β and N.

β	**N**	L^*	D_x^*	D_y^*	D_x^* / L^*	D_y^* / L^*
	0	1558.126128	4.479618	4.659037	0.002875	0.002990
	0.005	1553.541927	4.491265	4.653068	0.002891	0.002995
	0.01	1548.957685	4.503034	4.647071	0.002907	0.003000
0	0.06	1503.112113	4.627723	4.585606	0.003079	0.003051
	0.1	1466.429809	4.737194	4.534572	0.003230	0.003092
	0.25	1328.794584	5.237769	4.330494	0.003942	0.003259
	0.5	1098.978959	6.508453	3.966098	0.005922	0.003609
	0	1027.320520	4.538573	4.597709	0.004418	0.004475
	0.005	1024.789034	4.544459	4.597816	0.004435	0.004487
	0.01	1022.253897	4.550410	4.597931	0.004451	0.004498
0.5	0.06	996.709266	4.613613	4.599652	0.004629	0.004615
	0.1	976.035848	4.669373	4.601944	0.004784	0.004715
	0.25	896.934169	4.928311	4.622017	0.005495	0.005153
	0.5	761.838764	5.617123	4.735124	0.007373	0.006215
	0	769.445151	4.567997	-	0.005937	-
	0.005	767.593439	4.571012	-	0.005955	-
	0.01	765.738760	4.574063	-	0.005973	-
1	0.06	747.034901	4.606628	-	0.006167	-
	0.1	731.878710	4.635631	-	0.006334	-
	0.25	673.766753	4.774012	-	0.007086	-
	0.5	574.354866	5.167786	-	0.008998	-

Table 6. Load-carrying capacity and friction force components for R=2 and some values of β and N.

β	**N**	L^*	D_x^*	D_y^*	D_x^* / L^*	D_y^* / L^*
	0	2.102938	0.167103	0.233692	0.079462	0.111127
	0.005	2.050874	0.163591	0.222032	0.079767	0.108262
0	0.01	1.998683	0.160035	0.209926	0.080070	0.105032
	0.03	1.788049	0.145203	0.156366	0.081208	0.087451
	0.06	1.463035	0.121664	0.056389	0.083159	0.038543
	0	1.289173	0.186477	0.206596	0.144649	0.160254
	0.005	1.258748	0.180609	0.198290	0.143483	0.157529
0.5	0.01	1.227899	0.174556	0.189669	0.142159	0.154466
	0.03	1.100334	0.148132	0.151514	0.134625	0.137698
	0.06	0.899058	0.101024	0.081056	0.112366	0.090157
	0	0.958128	0.196142	-	0.204714	-
	0.005	0.935619	0.189105	-	0.202117	-
1	0.01	0.912771	0.181818	-	0.199194	-
	0.03	0.818058	0.149723	-	0.183023	-
	0.06	0.668241	0.091247	-	0.136549	-

the flow has the feature that the order of the system of differential equations exceeds the number of available boundary conditions. Nevertheless we have obtained the exact numerical solution by augmenting the boundary

Table 7. Load-carrying capacity and friction force components for *R*=5 and some values of β and *N*.

β	**N**	L^*	D_x^*	D_y^*	D_x^* / L^*	D_y^* / L^*
0	0	0.196668	0.012686	0.024616	0.064504	0.125163
	0.005	0.187432	0.008067	0.014642	0.043037	0.078122
	0.01	0.178061	0.003324	0.004725	0.018667	0.026534
0.5	0	0.114008	0.015558	0.018811	0.136465	0.165001
	0.005	0.108361	0.009575	0.011349	0.088361	0.104731
	0.01	0.102446	0.003534	0.003895	0.034497	0.038022
1	0	0.084340	0.017058	-	0.202252	-
	0.005	0.080146	0.010385	-	0.129580	-
	0.01	0.075744	0.003689	-	0.048697	-

conditions at $\eta = 0$. The resulting boundary value problem has been solved numerically using the Matlab solver SBVP. The current numerical investigation is limited to values of cross-flow Reynolds number in the interval $0 \le R \le 5$. An excellent agreement of the present results with existing results has been shown. Hence, it is concluded that the Matlab solver SBVP is very powerful and efficient in finding the exact numerical solution of the boundary value problem discussed in this research. Numerical calculations have been carried out for various values given to the non-dimensional parameters and the significant contributions of the elastic parameter *N* to the lateral velocity components, load-carrying capacity and friction force components have been pointed out. In addition, it is shown that the perturbation solutions fail to give satisfactory results when $R > 1$ and $N > 0.2$.

ACKNOWLEDGEMENT

We would like to thank the editor and referees for their useful comments and suggestions regarding an earlier version of this paper.

REFERENCES

Ariel PD (1992). A hybrid method for computing the flow of viscoelastic fluids. Int. J. Numer. Meth. Fluids 14:757-774.
Ariel PD (1993). Flow of viscoelastic fluids through a porous channel – I. Int. J. Numer. Meth. Fluids 17:605-633.
Ariel PD (1995). A new finite difference algorithm for computing the boundary layer flow of viscoelastic fluids in hydromagnetics. Comput. Meth. Appl. Mech. Eng. 124:1-13.
Ariel PD (2002). On exact solutions of flow problems of a second grade fluid through two parallel porous walls. Int. J. Eng. Sci. 40:913-941.
Ariel PD (2002). On extra boundary condition in the stagnation point flow of a second grade fluid. Int. J. Eng. Sci. 40:145-162.
Ariel PD (2008). Two dimensional stagnation point flow of an elastico-viscous fluid with partial slip. Z. Angew. Math. Mech. 88:320-324.
Ariel PD, Teipel I (1994). On dual solutions of stagnation point flow of a viscoelastic fluid. Z. Angew. Math. Mech. 74:341-347.
Auzinger W, Kneisl G, Koch O, Weinmüller EB (2002). A solution routine for singular boundary value problems. Techn Rep ANUM Preprint No 1/02. Depart Appl Math Num Analy, Vienna University of Technology, Austria.
Barış S (2002). Steady flow of a Walter's B viscoelastic fluid between a porous elliptic plate and the ground. Turk. J. Eng. Environ. Sci. 26:403-418.
Barış S, Dokuz MS (2006). Three-dimensional stagnation point flow of a second grade fluid towards a moving plate. Int. J. Eng. Sci. 44:49-58.
Beard DW, Walters K (1964). Elastico-viscous boundary layer flows. Part I: Two-dimensional flow near a stagnation point. Proc. Camb. Phil. Soc. 60:667-674.
Berman AS (1953). Laminar flow in channels with porous walls. J. Appl. Phys. 24:1232-1235.
Bhatt BS (1981). The elliptic porous slider at low cross-flow Reynolds number using a non-Newtonian second-order fluid. Wear 71:249-253.
Brady JF (1984). Flow development in a porous channel and tube. Phys. Fluids 27:1061-1067.
Bujurke NM, Madalli VS, Mulimani BG (2000). Laminar flow in a uniformly porous tube. Indian J. Pure Appl. Math. 31:341-352.
Choi JJ, Rusak Z, Tichy JA (1999). Maxwell fluid suction flow in a channel. J. Non-Newton Fluid Mech. 85:165-187.
Cox SM (1991). Two dimensional flow of a viscous fluid in a channel with porous walls. J. Fluid Mech. 227: 1-33.
Davies RT (1967). Boundary layer theory for viscoelastic liquids. In: Proceedings of the 10th Midwestern Mechanics Conference, Colorado, pp. 1145-1161.
Elsharkawy AA, Alyaqout SF (2009). Optimum shape design for surface of a porous slider bearing lubricated with couple stress fluid. Lubr. Sci. 21:1-12.
Fang T (2004). A note on the incompressible couette flow with porous walls. Int. Commun. Heat Mass Transf. 31:31- 41.
Faraz N (2011). Study of the effects of the Reynolds number on circular porous slider via variational iteration algorithm-II. Compt. Math. Appl. 61:1991-1994.
Frater KR (1970). On the solution of some boundary value problems arising in elasticoviscous fluid mechanics. Z. Angew. Math. Phys. 21:134-137.
Garg VK (1994). Heat transfer due to stagnation point flow of a non-Newtonian fluid. Acta Mech. 104:159-171.
Ghasemi E, Bayat M (2011). Viscoelastic MHD flow of Walters liquid B fluid and heat transfer over a non-isothermal stretching sheet. Int. J. Phys. Sci. 6:5022-5039.
Ghoreishi M, Md. Ismail AIB, Rashid A (2012). The one step optimal homotopy analysis method to circular porous slider (Article ID 135472). Math. Prob. Eng. 2012:1-14.
Gupta U, Aggarwal P (2011). Thermal instability of compressible

Walters' (Model B) fluid in the presence of Hall currents and suspended particles. Ther. Sci. 15:487-500.
Joneidi AA, Domairry G, Babaelahi M (2010). Homotopy analysis method to Walter's B fluid in a vertical channel with porous wall. Meccanica 45:857-868.
Kamisli F (2006). Laminar flow of a non-Newtonian fluid in channels with wall suction or injection. Int. J. Eng. Sci. 44:650-661.
Keith TG, Cioc S, Moraru L (2012). Hydrodynamic step and wedge bearings. In: R. W. Bruce (Ed.), Handbook of Lubrication and Tribology, Vol. II, CRC Press, New York.
Khan Y, Faraz N, Yıldırım A, Wu Q (2011a). A series solution of the long porous slider. Tribol. Trans. 54: 187-191.
Khan Y, Wu Q, Faraz N, Yıldırım A, Mohyud-Din ST (2011b). Three dimensional flow arising in the long porous slider: An analytic solution. Z. Naturforsch. 66a:507-511.
Kurtcebe C, Erim MZ (2005). Heat transfer of a viscoelastic fluid in a porous channel. Int. J. Heat Mass Transf. 48: 5072-5077.
Mustafa N, Asghar S, Hossain MA (2008). Natural convection flow of second-grade fluid along a vertical heated surface with power-law temperature. Chem. Eng. Comm. 195:209-228.
Nandeppanavar MM, Abel MS, Tawade J (2010). Heat transfer in a Walter's liquid B fluid over an impermeable stretching sheet with non-uniform heat source / sink and elastic deformation. Commun. Nonlin. Sci. Numer. Simul. 15:1791-1802.
Prakash OM, Kumar D, Dwivedi YK (2012). Heat transfer in MHD flow of dusty viscoelastic (Walter's liquid model-B) stratified fluid in porous medium under variable viscosity. Pramana-J. Phys. 79:1457-1470.
Proudman I (1960). An example of steady laminar flow at large Reynolds number. J. Fluid Mech. 9:593-602.
Sadeghy K, Najafi AH, Saffaripour M (2005). Sakiadis flow of an upper-convected Maxwell fluid. Int. J. Non-Lin. Mech. 40:1220-1228.
Sadeghy K, Sharifi M (2004). Local similarity solution for the flow of a second-grade viscoelastic fluid above a moving plate. Int. J. Non-Lin. Mech. 39:1265-1273.
Schlichting H (1968). Boundary layer theory. McGraw-Hill, New York.
Sellars JR (1955). Laminar flow in channels with porous walls at high suction Reynolds number. J. Appl. Phys. 26:489-490.
Shah RC, Parsania MM, Kataria HR (2012). Lubrication of isotropic permeable porous inclined slider bearing with slip velocity and squeeze velocity. Am. J. Fluid Dyn. 2:61-64.
Shukla S, Deheri G (2011). Surface roughness effect on the performance of a magnetic fluid based porous secant shaped slider bearing. Ind. Eng. Lett. 1:12-25.
Singh J, Gupta SK, Chandrasekaran S (2010). Computational treatment of free convection effect on flow of elastico-viscous fluid past an accelerated plate with constant heat flux. Appl. Math. Comput. 217:685-688.
Singh KD (1993). Three dimensional viscous flow and heat transfer along a porous plate. Z. Angew. Math. Mech. 73: 58-61.
Skalak FM, Wang CY (1975). Fluid dynamics of a long porous slider. ASME J. Appl. Mech. 42:893-894.
Skalak FM, Wang CY (1978). On the nonunique solutions of laminar flow through a porous tube or channel. SIAM J. Appl. Math. 34:535-544.
Teipel I (1986). Die räumliche staupunktströmung für ein viscoelastisches fluid. Rheol. Acta. 25: 75-79.
Terrill RM, Shrestha GM (1965). Laminar flow through parallel and uniformly porous walls of different permeability. Z. Angew. Math. Phys. 16:470-482.
Tonekaboni SAM, Abkar R, Khoeilar R (2012). On the study of viscoelastic Walters' B fluid in boundary layer flows (Article ID 861508). Math. Prob. Eng. 2012:1-18.
Wang CY (1974). Fluid dynamics of the circular porous slider. ASME J. Appl. Mech. 41:343-347.
Wang CY (1978). The elliptic porous slider at low crossflow Reynolds numbers. ASME J. Lubr. Technol. 100: 444-446.
Wang CY (2012). A porous slider with velocity slip. Fluid Dyn. Res. 44:1-14.
Watson LT, Li TY, Wang CY (1978). Fluid dynamics of the elliptic porous slider. ASME J. Appl. Mech. 45:435-436.
White FM, Barfield BF, Goglia MJ (1958). Laminar flow in a uniformly porous channel. ASME J. Appl. Mech. 25:613-617.
Yuan SW (1956). Further investigation of laminar flow in channels with porous walls. J. Appl. Phys. 27:267-269.